

Functional Nanoparticles

DOI: 10.1002/ange.200502517

Reactive Polymers: A Versatile Toolbox for the Immobilization of Functional Molecules on TiO₂ Nanoparticles**

Muhammad Nawaz Tahir, Marc Eberhardt,
Patrick Theato, Simon Faiß, Andreas Janshoff,
Tatiana Gorelik, Ute Kolb, and Wolfgang Tremel*

The nanoengineering of particle surfaces is a key for the design and tailored construction of innovative nanomaterials.^[1] To have control of the inorganic nanoparticle surfaces allows one to tailor the particle size^[2] and solubility.^[3] Moreover, the surface characteristics of nanomaterials influence the broad range of properties and the performance of a large variety of devices. For instance, the charge-transport process across the interface between a semiconductor metal oxide and an organic dye^[4] or a biomolecule^[5] forms the basis for improving the performance of many optoelectronic devices, photovoltaic cells,^[6] and light-emitting diodes (LEDs).^[7] Oligonucleotides can also be linked to the surfaces of nanoparticles, which may become a new tool for gene

[*] M. N. Tahir, Prof. Dr. W. Tremel
Institut für Anorganische Chemie und Analytische Chemie
Johannes Gutenberg-Universität
Duesbergweg 10–14, 55099 Mainz (Germany)
Fax: (+49) 6131-39-25605
E-mail: tremel@uni-mainz.de

M. Eberhardt, Dr. P. Theato
Institut für Organische Chemie
Johannes Gutenberg-Universität
Duesbergweg 10–14, 55099 Mainz (Germany)

S. Faiß, Prof. Dr. A. Janshoff, Dr. T. Gorelik, Dr. U. Kolb
Institut für Physikalische Chemie
Johannes Gutenberg-Universität
Welderweg 11, 55099 Mainz (Germany)

[**] This work was supported by the Deutsche Forschungsgemeinschaft (DFG) through SFB 625.



Supporting information for this article is available on the WWW under <http://www.angewandte.org> or from the author.

therapy.^[8] To conjugate inorganic nanomaterials to organic moieties in hybrid materials by strong covalent or ionic interactions, reactive organic groups have to be attached on the surface of the inorganic component.^[9] Surface modification of nanomaterials can be achieved by two methods: by grafting organic groups to the surface of nanomaterials after synthesis (post-functionalization)^[10] or by the modification of nanomaterials in situ by organic compounds (in situ functionalization).^[11]

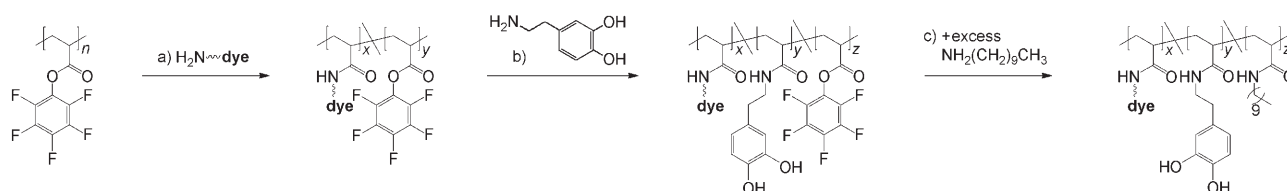
Nanocrystalline TiO₂ is particularly attractive for several applications, such as photocatalysis,^[12] solar cells,^[13] membranes,^[14] sensors,^[15] nanoceramics,^[16] and the degradation of environmental hazardous chemicals.^[17] Herein, we introduce a new versatile polymeric ligand that can be used for both the post- and in situ functionalization of TiO₂ as well as other metal oxide nanomaterials.^[18] The multifunctional polymeric ligand combines three features: 1) a robust anchor group based on dopamine which is capable of binding to many metal oxides (e.g. TiO₂, Fe₂O₃),^[19] 2) a functional molecule (e.g. fluorescent dye, catalyst, biomolecule), and 3) a group that provides solubility of the nanoparticle in different solvents and thereby allows various applications of the inorganic nanomaterial (e.g. solubility of TiO₂ pigments, directed binding to biological targets). The architecture of the polymeric ligand is of major importance because it provides the basis of a comprehensive toolbox to construct supramolecular assemblies of organic–inorganic hybrid nanomaterials. Moreover, this strategy of functionalization can be extended by introducing suitable anchor groups for nanomaterials other than metal oxides.^[20a]

The fact that active ester polymers react fast and quantitatively with amines to form the corresponding polyacrylamides opens the possibility to obtain multifunctional polymeric materials.^[19] Active ester polymers based on pentafluorophenylacrylates exhibit some outstanding features compared to the commonly used poly(*N*-hydroxysuccinimideacrylates), such as better solubility and higher reactivity, as described elsewhere.^[20b] The synthesis of the multifunctional polymeric ligand starting from the precursor pentafluorophenylacrylate polymer is shown in Scheme 1. The active ester ligand was prepared by free-radical polymerization to yield a polymer with a number-average molecular mass $M_n = 29.7 \text{ kg mol}^{-1}$ and weight-average molecular mass $M_w = 58.5 \text{ kg mol}^{-1}$ (polydispersity index, PDI = 1.96). This prepolymer was then transformed into the multifunctional polymeric ligand by substituting with amine-containing functionalities. Polymers **P1**, **P2**, and **P3** were prepared by a stepwise substitution of the active ester groups, first, by

addition of fluorescent dyes (1-pyrenemethylamine (PyMA), piperazinyl-4-chloro-7-nitrobenzofurazane (pipNBD), and Texas Red, respectively), second, by reaction with 3-hydroxytyramine anchor groups, and last, by quenching with decylamine. The resulting polymer thus incorporates three different features: 1) a fluorescent dye as a functional demonstrator molecule, 2) 3-hydroxytyramine as anchor groups for attachment onto the metal oxide nanoparticles, and 3) a long alkyl chain to increase solubility in nonpolar solvents. The multifunctional polymers thus obtained were analyzed by ¹H NMR and FTIR spectroscopy and GPC to determine the composition of the polymers. The amount of dye and 3-hydroxytyramine, respectively, within the polymers **P1**, **P2**, and **P3** was determined as 10 mol % each. The remaining 80 mol % of the polymers comprised *N*-decylacrylamide repeating units.

For the in situ functionalization of the TiO₂ nanocrystals, TiCl₄ was injected into the solution of the polymeric ligand in benzyl alcohol. The solution was stirred for two days at 80 °C under argon atmosphere. Post-functionalization was achieved by sealing a mixture of TiO₂ nanowires (synthesized from conc. NaOH and titanium 2-propoxide) and 10 mL of polymeric ligand in benzyl alcohol. In both cases, the product was repeatedly washed with CH₂Cl₂ to remove any unconverted ligand. The functionalized TiO₂ nanocrystals were characterized by transmission electron microscopy (TEM), X-ray diffraction (XRD), ¹H NMR spectroscopy, confocal laser scanning microscopy, and fluorescence spectrophotometry.

TEM images of the synthesized TiO₂ nanowires and TiO₂ nanoparticles are shown in Figure 1. An overview of the nanowires, which were used for post-functionalization, is given in Figure 1a. Figure 1b and c show the TEM images of the in situ functionalized TiO₂ nanoparticles (using **P1**, **P2**, and **P3**) at low magnification and high resolution, respectively. At low magnification (Figure 1b) it can be seen that the sample consists almost exclusively of nanometer-sized TiO₂ particles arranged in a partly agglomerated fashion on a TEM grid.^[21] Although it is difficult to identify individual isolated TiO₂ particles because of the presence of the polymeric ligand, a high-resolution (HR)TEM image of an isolated particle is presented in Figure 1c. The crystallinity and phase of the as-synthesized TiO₂ nanoparticles were confirmed by XRD (Figure 2) and TEM (see inset of Figure 1c), which revealed the characteristic diffraction patterns of anatase. Figure 1c shows the HRTEM image of a nanoparticle (diameter $d \approx 2 \text{ nm}$, length $l \approx 12 \text{ nm}$) along the [100] view together with the fast Fourier transform (FFT) in the lower right corner. The distances calculated are in good agreement



Scheme 1. Stepwise synthesis of the multifunctional polymeric ligands, which contain 3-hydroxytyramine as anchors for the nanoparticles, alkyl chains for solubility, and fluorescent dye molecules. The active ester units of the polymers were exchanged by 1-pyrenemethylamine in **P1**, pipNBD in **P2**, and Texas Red in **P3**.

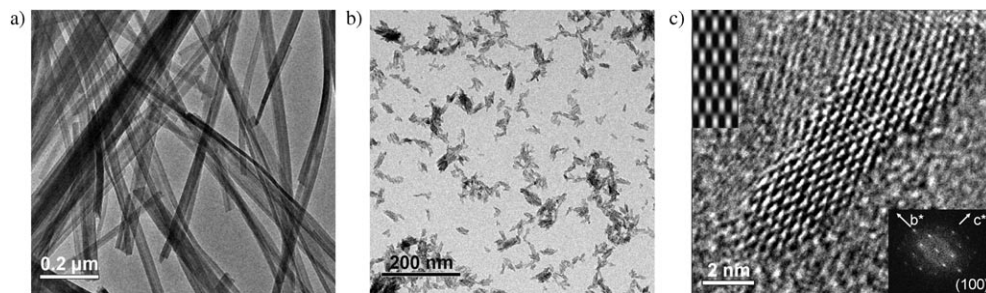


Figure 1. Transmission electron micrographs of a) synthesized TiO₂ nanowires, b) nanoparticles (overview image), and c) an individual nanoparticle (high resolution). The Fourier transform (FFT) and a theoretical HRTEM image of the [100] zone are shown in the lower right and upper left corners, respectively, of part (c).

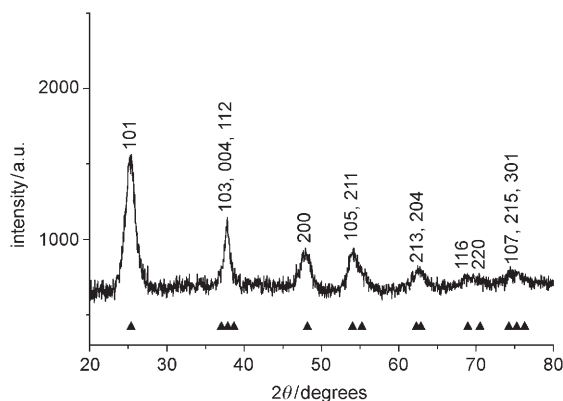


Figure 2. X-ray diffraction pattern of in situ functionalized TiO₂ nanoparticles. The pattern can be fully indexed to anatase. Indices of the reflections are provided, and calculated positions of the anatase reflections are indicated (▲).

with the theoretical values of anatase reflection of the [100] zone ($d_{\text{exp}}/d_{\text{theo}}$ [Å]: (011) = 3.57/3.51; (004) = 2.40/2.38; (020) = 1.94/1.89). The theoretical HRTEM image of the [100] zone (shown in the upper left corner) was calculated by a multislice method for a thickness of 2 nm at the Scherzer focus and resembles well the experimentally derived image. The crystallinity and the morphology of the TiO₂ nanoparticles are independent of the polymeric ligand **P1**, **P2**, or **P3** used in the synthesis.

The XRD pattern of the as-synthesized polymer-functionalized TiO₂ nanoparticles is shown in Figure 2. All reflections could be indexed to anatase with (101) as the strongest reflection (the calculated reflection positions are highlighted with ticks on the abscissa for comparison). The width of the (004) peak in comparison to the (101) reflection is indicative of the preferred growth of the particle along the *c* direction. In the powder pattern, no traces of other TiO₂ polymorphs could be detected; that is, the crystalline material can be considered a single phase. The peak broadening is due to the nanosized particles. Pawley fitting^[22] of the XRD data combined with Scherrer's formula^[23] delivered a particle size of 2 nm in both the

a and *b* directions and 12 nm in the *c* direction. This is in good agreement with the particle shown in Figure 1c. Note that all particles exhibit a good crystallinity, despite the low reaction temperature of 80 °C and the presence of the chelating ligand (10% dopamine).

Figure 3 shows the confocal laser scanning microscopy images of TiO₂ nanowires and nanoparticles after functionalization of the surface with **P2** and **P3**, respectively. Overview images of as-functionalized TiO₂ nanowires with polymeric ligands

P2 and **P3** are shown in Figure 3a and e, while a single isolated nanowire can be seen in Figure 3b and f. The corresponding nanoparticles functionalized in situ with polymeric ligands **P2** and **P3** are shown in Figure 3d and h, respectively. It is clear from the fluorescence profiles (Figure 3c and g) and images that the nanowires are fully coated by polymer ligands covalently bound to TiO₂ nanowires. The in situ functionalized TiO₂ nanoparticles shown in Figure 3d and h also exhibit the corresponding fluorescence. It is difficult to comment on the actual size of the in situ functionalized nanoparticles because it was beyond the resolution limits of confocal laser scanning microscopy. TiO₂ nanocrystals with surface-bound dopamine have been used for biotin–avidin functionalization coupling. Dopamine binding is a standard method for the surface functionalization of metal oxides^[20] where the dopamine group preferentially binds to the edges of the TiO₂ nanocrystals (which have a higher surface energy).^[5a] In contrast, full surface coverage, protection, and concomitant functionalization can be achieved by using the novel copolymer ligand which contains a large number of dopamine groups covalently linked to the polymer backbone, whereby the nanoparticles are sheathed partly by surface-bound anchor groups and partly by steric shielding through the polymeric ligand.

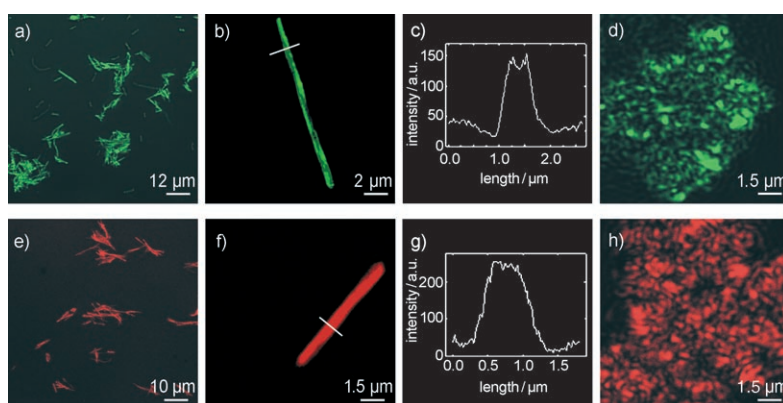


Figure 3. Confocal laser scanning microscopy images and fluorescence profiles of TiO₂ nanowires and nanoparticles. a, b) Post-functionalized TiO₂ nanowires coated with **P2** (NBD), c) the corresponding fluorescence profile for an individual nanowire, and d) TiO₂ nanoparticles functionalized in situ with **P2**. e, f) Post-functionalized TiO₂ nanowires coated with **P3** (Texas Red), g) the corresponding fluorescence profile for an individual nanowire, and h) TiO₂ nanoparticles in situ functionalized with **P2**.

The versatile use of the functional polymeric ligands as immobilizers for metal oxide nanowires and nanoparticles was demonstrated by the attachment of the three different fluorescent dyes: pyrene in **P1**, NBD in **P2**, and Texas Red in **P3**. To detect the immobilization of the functional polymers on the TiO₂ surfaces, fluorescence spectra were measured. Figure 4a shows the fluorescence spectra of TiO₂ nano-

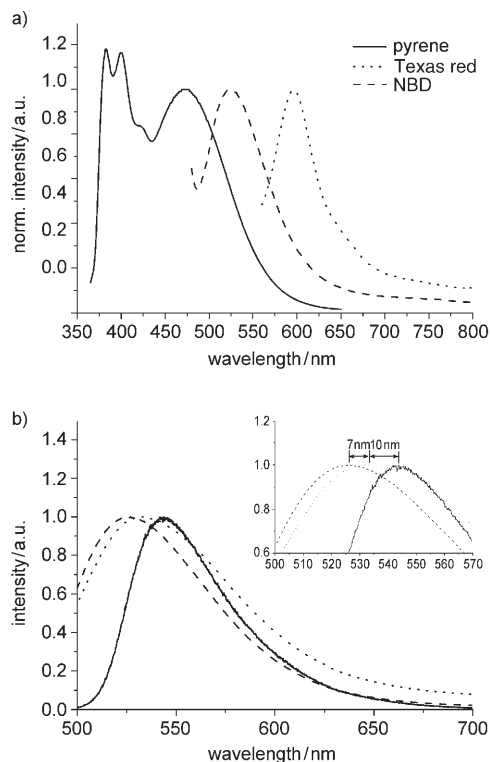


Figure 4. a) Fluorescence spectra of TiO₂ nanoparticles coated with **P1** (pyrene; $\lambda_{\text{ex}} = 345$ nm), **P2** (NBD; $\lambda_{\text{ex}} = 460$ nm), or **P3** (Texas red; $\lambda_{\text{ex}} = 488$ nm). b) Fluorescence spectra of NBD depending on the preparation conditions: post-functionalization (red dotted line); in situ functionalization (blue dashed line); the emission spectrum of **P2** dissolved in CHCl₃ (black solid line) was used as a reference. The inset shows the extent of the blue shifts of the maxima relative to that of the reference.

particles coated with **P1** (solid line), **P2** (dashed line), or **P3** (dotted line). All samples were dissolved in CHCl₃ for measurement of their emission spectra (see Supporting Information). TiO₂ nanoparticles carrying the **P1** pyrene fluorophore were excited at 345 nm, those coated with **P2** were excited at 460 nm, and those derivatives with **P3** were excited at 488 nm. Clearly, the expected emission spectra of the respective dye can be seen which proves the flexible application of the functional polymeric ligands.

As the functional polymeric ligands were used for both post- and in situ functionalization of TiO₂ nanoparticles, we investigated the fluorescence of **P2** depending on the synthetic procedure (Figure 4b). The solid line in Figure 4 shows the emission spectrum of **P2** dissolved in CHCl₃ as a reference. TiO₂ nanowires that were coated with **P2** show a fluorescence spectrum whose maximum is blue-shifted by 10 nm relative to that of the reference, whereas the emission

maximum of TiO₂ nanoparticles that were synthesized in the presence of the polymeric ligand **P2** revealed a blue shift of 17 nm with respect to **P2**. This can be understood as follows: The nanoparticles are coated with the polymer which results in a non-uniform environment for the dye molecules. As a result, the hydrophilic TiO₂ surface induces a slight blue shift. This also explains the larger blue shift for the in situ functionalized nanoparticles than for the post-functionalized nanowires, as the nanoparticles exhibit a larger surface-to-volume ratio.

In conclusion, we have demonstrated for the first time that reactive polymer ligands containing dopamine serve as a robust anchor on the surface of titanium dioxide nanoparticles. Compared to the binding of molecules to the surface of oxide particles using dopamine, the novelty and superiority of the polymeric ligand system presented here is based on its multifunctionality, as it incorporates metal-chelating ligands, a functional molecule (pyrene, NBD, or Texas Red), and additional entities that allow the solubility of inorganic nanocrystals in different organic solvents to be tailored according to various potential applications. As a possible extension of the work presented, we envisage the immobilization of proteins to metal oxide surfaces using nitrilotriacetic acid as an anchor ligand;^[24] that is, our simple strategy should provide a useful way to link biofunctional molecules in almost any solvent to the surface of metal oxide particles that display a high affinity toward dopamine or toward any other linker group that can replace the dopamine ligand in the polymer. This strategy is extremely versatile and offers new opportunities for optoelectronic and/or biological applications of metal oxide nanoparticles. Finally, this strategy allows the construction of supramolecular structures through the arrangement of inorganic nanoparticles, for example, by introducing biotin/streptavidin linker units as the functional molecules.

Experimental Section

Piperazinyl-NBD (pipNBD) was synthesized according to a reported procedure^[1] by reaction of NBD chloride (Fluka) with an excess of piperazine in THF. 1-Pyrenemethylamine hydrochloride (PyMA) and Texas Red are commercially available (Aldrich).

The active ester polymer, poly(pentafluorophenylacrylate) (PFA) was prepared as reported previously.^[20b] GPC analysis of the obtained polymer (THF, light-scattering detection) gave the values $M_n = 29.7$ kg mol⁻¹ and $M_w = 58.5$ kg mol⁻¹; the number of repeating units (246) is based on the M_w value.

For the synthesis of the multifunctional poly(acrylamide)s, PFA (700 mg, 2.94 mmol repeating units) was dissolved in a mixture of dry DMF (9 mL) and triethylamine (0.7 mL). The calculated amount of dye dissolved in dry DMF was added, and the resulting solution was stirred for 4 h at 50 °C. 3-Hydroxytyramine hydrochloride (57 mg, 0.3 mmol) in DMF (3 mL) and triethylamine (1 mL) were added, and the clear solution was kept for 2 h at 50 °C. The remaining active ester groups were then quenched with an excess of decylamine (500 mg, 3.2 mmol). The polymer was isolated by precipitation in methanol and finally dried in a vacuum oven at 40 °C for 1 h.

A sample of the functional polymer ligand (100 mg) was dissolved in benzyl alcohol (20 mL) in a glovebox, and the vial was sealed and removed from the glovebox. TiCl₄ (0.8 mL) was slowly injected through the septum to the solution of ligand in benzyl alcohol under vigorous stirring at room temperature. With continuous stirring the

solution was heated to 80°C for 24 h. The resulting brown suspension was centrifuged, and the precipitate was thoroughly washed twice with CH₂Cl₂. The product was dried in air at room temperature.

Analytical grade ethanol (99.8%; 6 mL) was added to titanium 2-propoxide (ACROS; 1 g) in a teflon vessel, and the vessel was placed in a desiccator. The precipitation of TiO₂ was initiated under a moist atmosphere, induced by placing a petri dish filled with water at the bottom of the desiccator. The diffusion experiment was stopped after 12 h, and was followed by the addition of 10 M aqueous NaOH solution (25 mL). The reaction vessel was then sealed into a stainless steel hydrothermal bomb, which was placed in an oven maintained at 160°C for 20 h. After the autoclave was allowed to cool to room temperature, the obtained sample was filtered and repeatedly washed with 0.1 M HNO₃, 1 N HCl, and deionized water. The product was dried under vacuum for 3 h. Finally a soft, fibrous white powder was obtained. Then, TiO₂ nanowires (10 mg) were dispersed in benzyl alcohol (10 mL), and the mixture was sonicated for 15 min. In a separate vial, the polymer ligand (10 mg) was dissolved in benzyl alcohol (10 mL). Both the suspension and solution were mixed under inert conditions, and the mixture was stirred at 60°C for 4 h. The polymer-functionalized nanowires were isolated and purified by repeated washings with CH₂Cl₂ using centrifugation.

For confocal laser scanning microscopy 10 µL of the sample was placed and dispersed carefully on a thin glass slide washed in piranha solution, and the solvent was evaporated. NBD-functionalized nanowires were imaged using an argon laser with an excitation wavelength of 488 nm, whereas those functionalized with Texas Red were excited with the 543 nm line of a helium/neon laser. A 40× (NA: 1.25) oil immersion objective was used for the imaging of all samples.

Instrumentation: The resulting products were characterized by an inverted laser scanning microscope (Leica TCS SL, Leica Microsystems, Bensheim, Germany), X-ray powder diffraction in reflection geometry (Siemens D8 powder diffractometer, Cu_{Kα} radiation), HRTEM (Philips TECNAI F30 electron microscope; field-emission gun, 300 kV extraction voltage) equipped with a high-angle annular dark-field detector (HAADF), a Gatan imaging filter, and an energy dispersive X-ray analysis system.

Received: July 19, 2005

Revised: August 24, 2005

Published online: December 28, 2005

Keywords: fluorescence · nanostructures · organic–inorganic hybrid composites · polymers · titanium

- [10] G. Kickelbick, U. Schubert in *Synthesis, Functionalization and Surface Treatment of Nanoparticles* (Ed.: M.-I. Baraton), American Scientific, Stevenson Ranch, CA, **2003**.
- [11] a) C. Sanchez, G. Soler-Illia, F. Ribot, T. Lalot, C. R. Mayer, V. Cabuil, *Chem. Mater.* **2001**, *13*, 3061–3083; b) M. Anderson, L. Österlund, S. Ljungström, A. Palmqvist, *J. Phys. Chem. B* **2002**, *106*, 10674–10679; c) S. Yin, Y. Aita, M. Komatsu, J. Wang, Q. Tang, S. Sato, *J. Mater. Chem.* **2005**, *15*, 674–682.
- [12] S. Hore, E. Palomares, H. Smit, N. J. Bakker, P. Comte, P. Liska, K. R. Thampi, J. M. Karoon, A. Hinsh, J. R. Durrant, *J. Mater. Chem.* **2005**, *15*, 412–418.
- [13] A. Hagfeldt, M. Grätzel, *Acc. Chem. Res.* **2000**, *33*, 269–277.
- [14] B. S. Lele, A. J. Russell, *Biomacromolecules* **2004**, *5*, 1947–1955.
- [15] E. Palomares, R. Vilar, A. Green, J. R. Durrant, *Adv. Funct. Mater.* **2004**, *14*, 111–115.
- [16] “Nanocrystalline Ceramics, Synthesis and Structure”: M. Winterer, *Springer Series in Materials Science, Vol. 53*, Springer, Heidelberg, **2002**.
- [17] a) J. H. Schattka, D. G. Shchukin, J. G. Jia, M. Antonietti, R. A. Carusa, *Chem. Mater.* **2002**, *14*, 5103–5108; b) L. X. Chen, T. Rajh, Z. Y. Wang, M. C. Thurnauer, *J. Phys. Chem. B* **1997**, *101*, 10688–10697.
- [18] a) J. L. Dalsin, L. Lin, S. Tosatti, J. Vörös, M. Textor, P. B. Messersmith, *Langmuir* **2005**, *21*, 640–646; b) H. Gu, Z. Yang, J. Gao, C. K. Chang, B. Xu, *J. Am. Chem. Soc.* **2005**, *127*, 34–35.
- [19] N. M. Dimitrijevic, Z. V. Saponjic, B. M. Rabatic, T. Rajh, *J. Am. Chem. Soc.* **2005**, *127*, 1344–1345.
- [20] a) I. Potavova, R. Mruk, S. Prehl, R. Zentel, T. Basche, A. Mews, *J. Am. Chem. Soc.* **2003**, *125*, 320–321; b) M. Eberhardt, R. Mruk, P. Theato, R. Zentel, *Eur. Polym. J.* **2005**, *41*, 1569–1575.
- [21] TiO₂ nanoparticles that were functionalized in a similar manner have been shown by light-scattering experiments to have a hydrodynamic radius of approximately 80 nm, which is indicative of a partial agglomeration in solution and compatible with the slight agglomeration observed in the TEM image in Figure 1b.
- [22] Cerius2, Version 4.2MS, Accelrys Software Inc..
- [23] P. Scherrer, *Gött. Nachr.* **1918**, *2*, 98.
- [24] a) M. N. Tahir, P. Théato, W. E. G. Müller, H. C. Schröder, A. Janshoff, J. Zhang, J. Huth, W. Tremel, *Chem. Commun.* **2004**, 2848–2849; b) M. N. Tahir, P. Théato, W. E. G. Müller, H. C. Schröder, A. Borejko, S. Faiß, A. Janshoff, J. Huth, W. Tremel, *Chem. Commun.* **2005**, 5533–5535.

- [1] S. Banerjee, M. G. C. Kahn, S. S. Wong, *Chem. Eur. J.* **2003**, *9*, 1898–1908.
- [2] P. D. Cozzoli, A. Kornowski, H. Weller, *J. Am. Chem. Soc.* **2003**, *125*, 14539–14548.
- [3] K. Ausman, R. Piner, O. Lourie, R. S. Ruoff, M. D. Korobov, *J. Phys. Chem. B* **2000**, *104*, 8911–8915.
- [4] a) R. Nudelman, O. Ardon, Y. Hadar, Y. Chen, J. Libman, A. Shanzer, *J. Med. Chem.* **1998**, *41*, 1671–1678.
- [5] a) N. M. Dimitrijevic, Z. V. Saponjic, B. M. Rabatic, T. Rajh, *J. Am. Chem. Soc.* **2005**, *127*, 1344–1345; b) O. V. Salata, *J. Nanobiotechnology* **2004**, *2*–3, 1–6.
- [6] a) G. Ramakrishna, H. N. Ghosh, *J. Phys. Chem. B* **2001**, *105*, 7000–7008; b) W. J. E. Beek, R. A. J. Janssen, *J. Mater. Chem.* **2004**, *14*, 2795–2800; c) E. W. McFarland, J. Tang, *Nature* **2003**, *421*, 6, 616–618.
- [7] J.-W. Huang, S. J. Bai, *Nanotechnology* **2005**, *16*, 1406–1410.
- [8] T. Paunesku, T. Rajh, G. Wiederrecht, J. Maser, T. Vogt, N. Stojicevic, M. Protic, B. Lai, J. Oryhon, M. Thurnauer, G. Woloschak, *Nat. Mater.* **2003**, *2*, 343–346.
- [9] C. Xu, K. Xu, G. Gu, R. Zheng, H. Liu, X. Zhang, Z. Guo, B. Xu, *J. Am. Chem. Soc.* **2004**, *126*, 9938–9939.